

Convective Chemical Fronts in the 1,4-Cyclohexanedione–Bromate–Sulfuric Acid–Ferrioin System

Andrea Komlósi, István Péter Nagy,* and György Bazsa

Department of Physical Chemistry, Kossuth Lajos University, Debrecen, Hungary H-4010

John A. Pojman†

Department of Chemistry and Biochemistry, University of Southern Mississippi, Hattiesburg, Mississippi 39406-5043

Received: March 18, 1998; In Final Form: July 13, 1998

Traveling waves were investigated in the Belousov–Zhabotinsky reaction in which 1,4-cyclohexanedione was the substrate. Isothermal density change ($\Delta\rho_c$) and reaction enthalpy were determined. $\Delta\rho_c$ is positive, while the reaction enthalpy is negative; therefore, double-diffusive convection was expected according to the Pojman–Epstein model. Experiments were carried out in tubes and in spectrophotometric cells. In tubes the effect of the diameter and the orientation of the tube on the wave velocity and on the wave shape was studied; gravitational anisotropy and the expected double-diffusive convection were found. Experiments in cells were compared to the calculations of Wu et al. (Wu, Y.; Vasquez, D. A.; Edwards, B. F.; Wilder, J. W. *Phys. Rev. E* **1995**, *51*, 1119–1127). They predicted a critical cell width under which no simple convection should occur. However, because double-diffusive convection was observed, their calculations are not directly applicable.

Introduction

The propagation of chemical waves is due to the combination of an autocatalytic chemical reaction and diffusion. In many cases of propagating reaction fronts, the chemical reaction and the diffusion is not enough to describe the experimental results. In the presence of gravity the density gradients, created by the chemical waves, can destabilize planar reaction–diffusion waves. This leads to fluid convection.

The first systems in which this phenomenon was found were the iron(II)–nitric acid system and the chlorate–thiosulfite system. In the iron(II)–nitric acid system studied by Bazsa and Epstein,¹ the speed of the front was sensitive to the width of the tube and to the orientation with respect to gravity. The velocity of the propagating fronts was larger than that of the pure reaction–diffusion fronts. Nagypál et al.² investigated the chemical fronts in the chlorate–thiosulfate system and found that the front speed depends on the direction of propagation with respect to the gravitational vector.

Pojman and Epstein^{3–5} have classified the types of convection that can occur in chemical waves. They recognized that the overall density change is the sum of the thermally induced density change ($\Delta\rho_T$) and the isothermal density change caused by the change in composition ($\Delta\rho_c$). The relative signs of these values determine the type of convection. If the reaction is exothermic ($\Delta\rho_T < 0$) and the products' solution is less dense than the reactants' ($\Delta\rho_c < 0$), then *simple convection* can occur, depending on the constraints of the container geometry. In this case, the ascending front velocity is greater than or equal to that of the descending one, whose velocity is just the pure

reaction–diffusion velocity. The only fronts meeting this criterion are those in the iodate–arsenous acid system.^{4,6,7}

If the reaction is exothermic and the products' solution has a greater density than the reactants' ($\Delta\rho_c > 0$), then *multicomponent* (so-called *double-diffusive*) convection may occur. In a *descending front*, double-diffusive convection manifests itself as “salt fingers”, so-called because of their appearance in ocean layer mixing, while the *ascending front* is slightly curved. The most significant difference from simple convection is that both ascending and descending fronts are faster than the reaction–diffusion front, and descending fronts are generally faster than ascending fronts. This condition is relatively common, having been reported in many systems.^{1,2,8–12}

Convection in chemical waves, viz., with fronts periodically propagating through the medium, are less well-studied. Several works addressed the effect of convection in horizontally propagating waves with a free interface.^{13–19} We know of only two works on Belousov–Zhabotinsky (BZ) waves in a vertical reactor. The difficulty arises in the most commonly used system, catalyzed by ferrioin, from bubbles that rise and mix the solution. Menzinger et al. studied a bubble-free manganese-catalyzed variant in which magnetic resonance imaging was employed.²⁰ The $\Delta\rho_c$ is greater than zero, but very close to it. Thus ascending waves propagated faster than a descending one, in accord with the Pojman–Epstein model. The other work was done by Fujieda et al.²¹ They measured the speed of the traveling front in three directions: upward, horizontal, and downward. They found that the descending front is the fastest, while the ascending front is the slowest.

Several investigators have simulated the interaction of convection and BZ waves,^{22,23} but Wu et al.²⁴ have done the most realistic simulations. They used the Oregonator model in their calculations and assumed the $\Delta\rho_c < 0$. They found in the

* To whom correspondence should be addressed. E-mail: 3586nagy@tigris.klte.hu. FAX: +36 (52) 329-100#2591.

† E-mail: John.pojman@usm.edu.

case of ascending and descending waves that there is a critical slab width in each case under which convection does not appear. This differs from the analysis of simple convection in fronts because the solution does not consist of only two regions of differing density. Instead, the density varies periodically because of the periodic propagation of waves.

We wanted to test the simulations of Wu et al. and to determine the effect of orientation on the BZ waves, which no one has reported. For this purpose we chose the 1,4-cyclohexanedione (1,4-CHD)–bromate–sulfuric acid–ferroin system. (Ferroin is needed to visualize the occurrence and propagation of the wave front.) The reason for choosing this system was that in contrast to most of the BZ systems, in this system no gaseous product is formed. Although the manganese-catalyzed system employed by Menzinger et al. was also bubble free, they were required to use MRI to follow the fronts. This would make studying waves propagating at various orientations extremely difficult.

The 1,4-CHD–bromate–acid system belongs to the group of uncatalyzed bromate oscillators (UBOs). Most of the UBOs exhibit only a few, strongly damped oscillations under batch configuration. However, Farage and Janjic²⁵ reported 200–300 oscillations in the 1,4-CHD–bromate–acid system, and Kurin-Csörgei et al.²⁶ studied this system in detail. They examined chemical waves in this system in a thin layer.²⁷ Because aliphatic compounds were completely absent in the reaction mixture even in the later phase of the reaction, simple gaseous carbon compounds were not found among the reaction products. They also found that if the ferroin concentration is smaller than 5×10^{-5} M, then ferroin does not affect the oscillation period, the number of cycles, and the amplitude of oscillation of the redox potential. If it exceeds that concentration, the system behaves like a typical BZ system; i.e., the oscillation period increases approximately linearly with the concentration of ferroin.²⁸

Experimental Section

Chemicals and Apparatus. Reactant solutions were prepared with analytical grade chemicals that were used as received: 1,4-cyclohexanedione (1,4-CHD) from Aldrich, H₂SO₄ from Acidum Gmk (Debrecen, Hungary), (NH₄)₂Fe(SO₄)₂·6H₂O from Chemolab (Budapest), KBrO₃ and 1,10-Fenantrolin from Reanal (Budapest), and distilled water. 1,4-CHD was dissolved in 1 M H₂SO₄; then it was filtered. In each experiment the initial concentrations were the following: 0.1 M 1,4-CHD, 0.02 M KBrO₃, 2.5 M H₂SO₄, 5×10^{-4} M ferroin. Just after mixing the reactants, the solution became blue, and the product solution was red.

The experiments were carried out either in glass tubes (inside diameter: 0.9, 2.6, 3.9, 5.4, and 7.7 mm) or in Starna spectrophotometric glass cells (cell width: 0.1, 0.2, 0.5, and 1 mm). (By a cell we mean two slabs and the gap between them.) These tubes and cells were carefully cleaned and dried before each experiment, and at least three parallel experiments were done. In the case of the experiments realized in tubes, the wave position was read from a millimeter scale attached to the wall of the tube. Reaction enthalpies were determined using a Dewar flask and a Beckmann differential thermometer. Reaction mixture densities were measured in a 25 cm³ nominal pycnometer.

Batch experiments were also performed with the same initial concentrations, but the 10 cm³ volume of solution was stirred. The experiments were carried out in room temperature and under air. The potential of a smooth platinum electrode against a

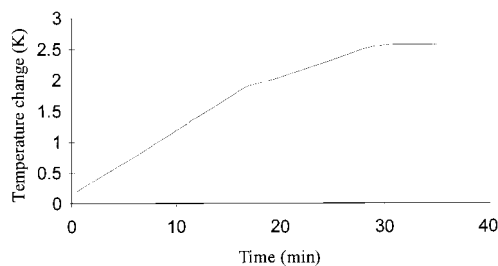


Figure 1. Calorimetric curve. Initial concentrations: 0.1 M 1,4-CHD; 0.02 M KBrO₃; 2.5 M H₂SO₄; 5×10^{-4} M ferroin.

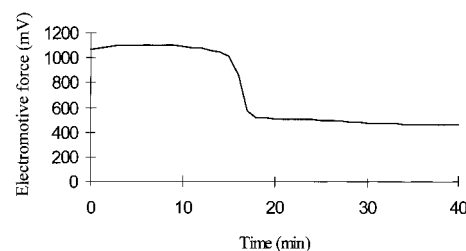


Figure 2. Batch experiment in the 1,4-CHD–bromate–ferroin–sulfuric acid system. Initial concentrations are the same as in Figure 1.

concentrated calomel electrode was measured with a Precision pH Meter (Type OP-205/1, Radelkis, Budapest).

Wave Velocity Measurements. Standard stock solutions and distilled water were pipetted in appropriate volumes to give reaction mixtures of the desired concentrations. After mixing the components, the tube or the cell was filled with the reaction mixture. In the case of tubes, they were attached to a plastic syringe with a rubber pipe, then the reaction mixture was pumped up, and the pipe was compressed. After an induction period of at least 15 min, a wave front began to propagate from the end of the cell in contact with the air. Wave shapes were captured by a digital image processing system that consisted of an IBM 80-486 compatible PC, an LFS-AT 8 bit black and white frame grabber board (Leutron AG, Switzerland), an SDT 4500 monochrome CCD solid-state camera (Steiner Datatechnik GmbH, Germany), and the necessary optics (25 mm focal length Tokina lenses, Japan). Recording was started 15 min after mixing of the components.

Experiments in Tubes. We examined the effect of tube orientation on the front velocity and shape and the effect of the tube diameter on the front velocity. The temperature was 24 ± 0.5 °C.

Experiments in Cells. We studied both ascending and descending waves. Because of the surface tension, the liquid remained in an inverted cell, if the width was sufficiently small. The experiments were executed at room temperature (24 ± 0.5 °C) in the case of waves moving down, and in the case of waves moving upward the temperature was 26–27 °C; therefore, the induction period was shorter in these experiments.

Determination of the Reaction Heat and the Isothermal Density Change. Appropriate volumes of stock solutions were combined to give a 200 cm³ reaction mixture that was then poured into a Dewar flask. The temperature change using 0.02 M initial bromate concentration of the reaction mixture was 2.75–2.8 °C, and the calculated reaction heat was -700 ± 30 kJ/mol. A typical calorimetric curve is presented in Figure 1.

The isothermal density change was determined under the same conditions as the wave velocity experiments using a 25 cm³ nominal volume pycnometer. The isothermal density change, $\Delta\rho_c$, was found to be $+5 \pm 10^{-5}$ g/cm³, between the initial oxidized state and the reduced state.

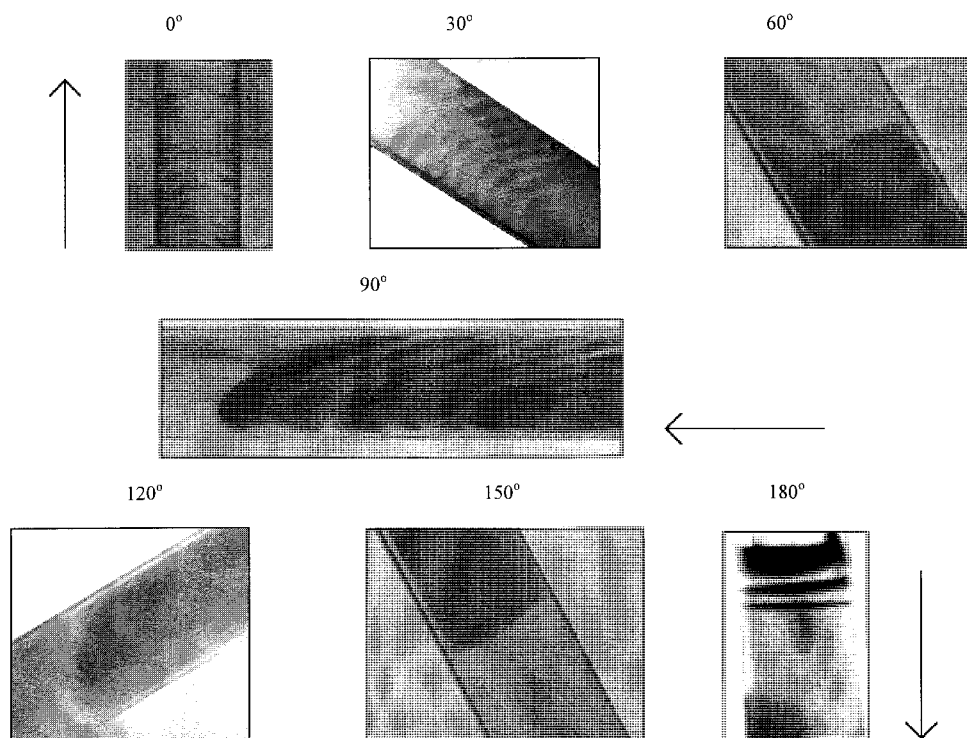


Figure 3. Shape of the waves formed in the 1,4-CHD–bromate–ferroin–sulfuric acid system: 0° , the vertical ascending direction; 180° , the vertical descending direction. Initial concentrations are the same as in Figure 1.

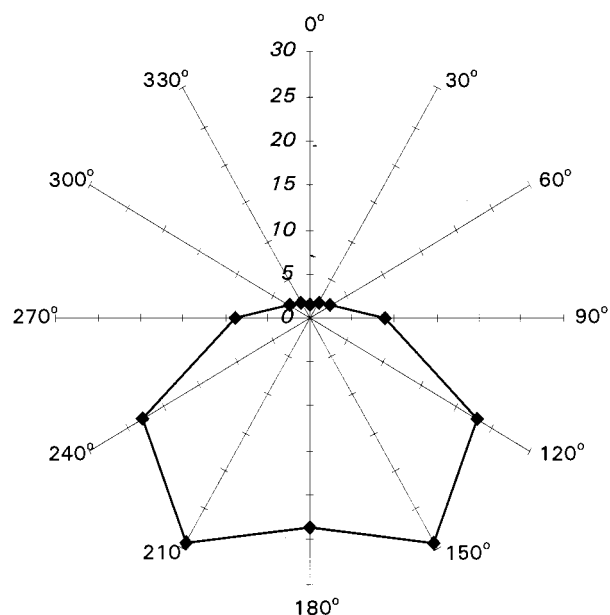


Figure 4. Polar coordinate plots of the front velocities (in millimeters per minute) versus tube orientations in a 3.9 mm tube: 0° , the vertical ascending direction; 180° , the vertical descending direction. Initial conditions are the same as in Figure 1.

Results

Batch Experiment. Figure 2 shows the electrode potential–time curve of the same initial concentrations that were used in the wave experiments. Within our circumstances no oscillation was observed. Kurin–Csörgei et al.²⁸ used other initial concentrations in their oscillation experiments. Comparing Figure 1 and Figure 2, we can say that the batch reaction finishes within approximately 40 min. The color change was the same as in the wave experiments; that is, when the components were mixed, it turned blue immediately and it became red as the reaction occurred.

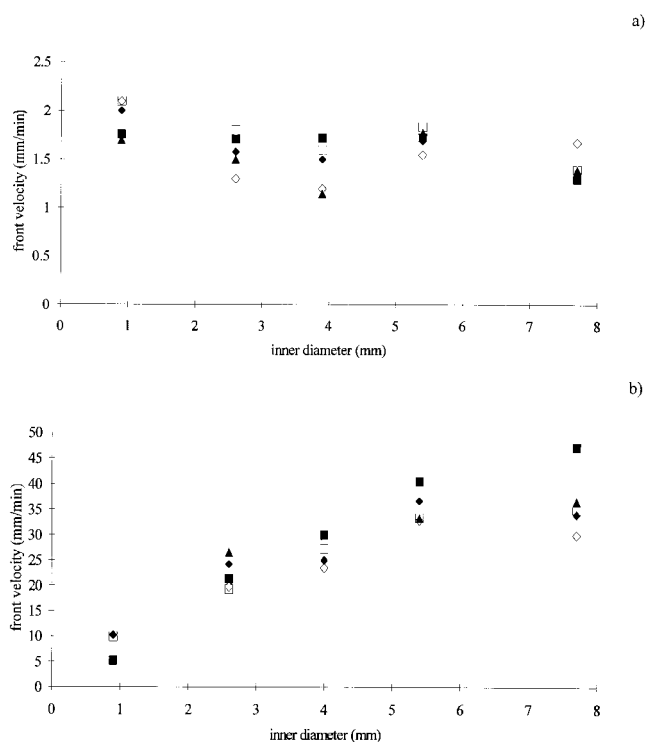


Figure 5. Diameter dependence of the front velocities in tubes. Initial conditions are the same as in Figure 1. (a) The front is moving upward. (b) The front is moving downward.

Wave Experiments in Tubes. After the induction period, a red chemical front started from the open end of the tube. The oxygen of the air can be necessary for the initiation of the reaction because the reaction front starts at the open end of the tube without any other initiation. The solution here becomes red (reduced), and this starts to propagate. After moving some millimeters, the solution behind the red front becomes blue again. Then red and blue stripes are formed in the product

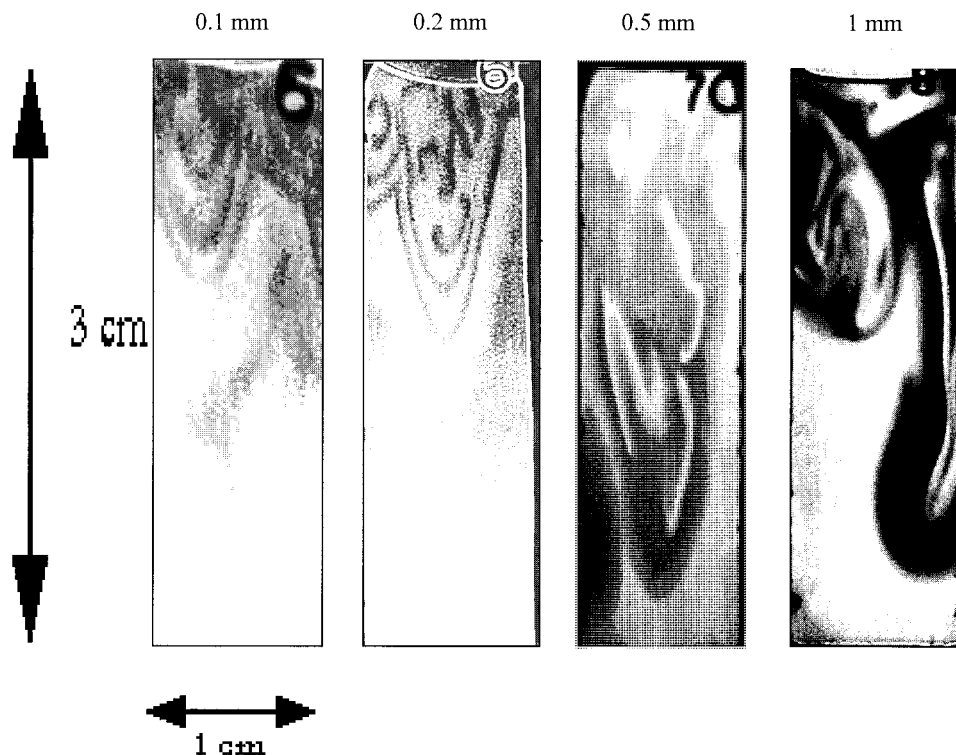


Figure 6. Shapes of propagating fronts moving downward at four different slab widths. The slab widths are shown above the pictures. The pictures were taken 3–4 min after the first 15 min. Initial conditions are the same as in Figure 1.

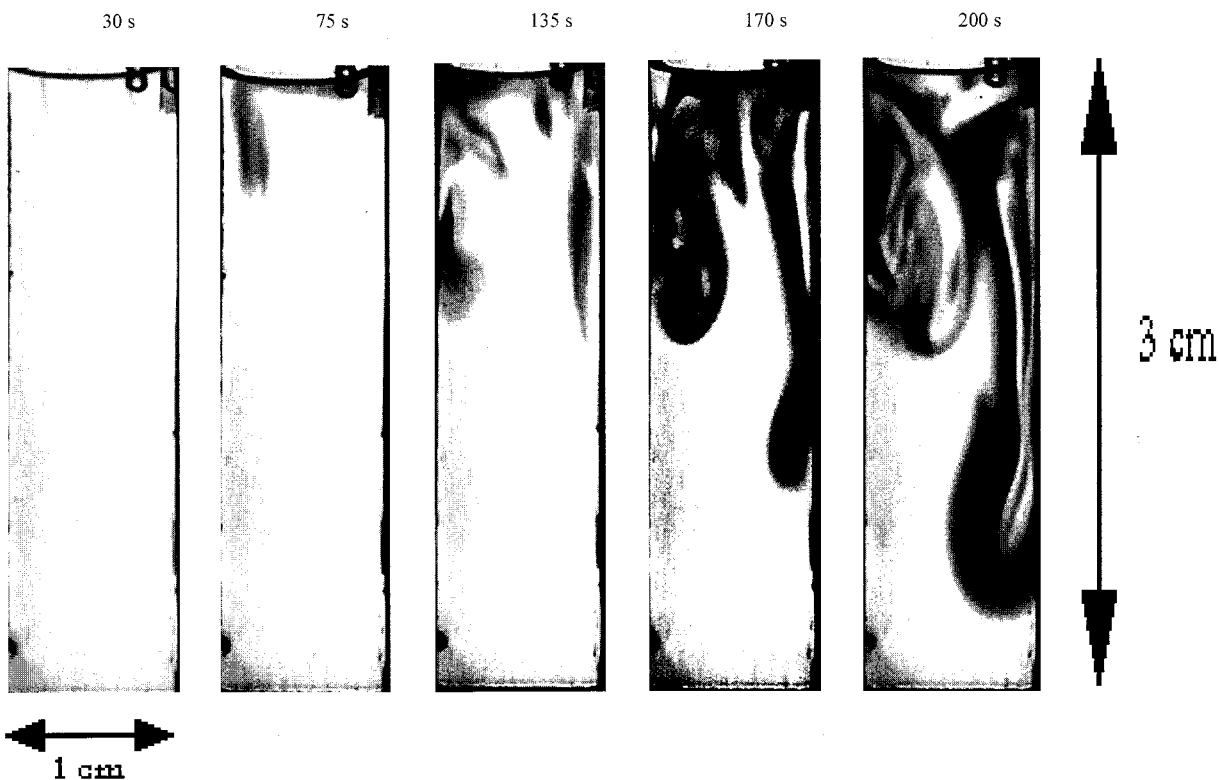


Figure 7. Formation of the chemical wave moving downward in a 1 mm wide slab. Time data appearing above the pictures indicate time (in seconds) passed after the first 15 min. Initial conditions are the same as in Figure 1.

solution. Some minutes later the stripes disappear, and the product solution is red.

Effect of Tube Orientation on Front Shape. Figure 3 shows the shape of the fronts. (Dark regions correspond to reduced solution, and light corresponds to oxidized.) The effect of convection can be seen in these pictures. Some of the pictures

show the stripes of the front, while the others were taken after the stripes disappeared.

Effect of Tube Orientation on Wave Velocity. The velocity of the first red stripe was measured. In all cases the wave velocity remained constant during the entire experiment. Using a 3.9 mm tube, we observed the gravitational anisotropy of front

Cell width (mm)	Induction period (minutes)	Time passed after the induction period (minutes)	Wave shape
0.1	8	5.25	
0.5	12	3	
1	12	4	

Figure 8. Shapes of propagating fronts moving upward at three different slab widths. Initial conditions are the same as in Figure 1.

velocities first discovered and described by Bazsa and Epstein¹ and also found in the chlorate–thiosulfate,² iodide–nitric acid,¹¹ iodate–sulfite,¹² and bromate–sulfite¹² systems. Figure 4 shows the result in different orientations in a 3.9 mm tube. An ascending wave is indicated by 0°, while a descending one is depicted at 180°. It is natural that the curve is left/right symmetric. The maximum velocity was found at 150°, which is consistent with the results found in the other systems cited above. The ascending front (0°) is very slow; its propagation speed is about 1.5 mm/min. If the tube is tilted a bit, but the reaction front propagates upward (30 and 60°), the velocity is 1.5–2 times larger. But in the case of the other experiments, the velocity increases much more. For example, the largest velocity (150°) is 20 times larger than the ascending front (0°). This is the first “pumpkin-shaped” diagram of a BZ system, the notion of which was first used by Nagypál et al.²

Effect of Tube Diameter on Wave Velocity. Figure 5 shows the variation of front velocities as a function of the inner diameter of the tube. The parallel experiments are also shown in the figure. In the case of fronts moving upward the tendency is not well-defined, but in the case of downward fronts the velocity increases with increasing tube diameter. It can also be seen that the values of the front velocities are at least 10 times larger downward than upward.

Wave Experiments in Open Cells. When the experiments were performed in the cells, after the induction period first a thin layer of product solution was formed at the open end of the cell and then a front curved like a finger appeared.

Descending Fronts. Figure 6 shows images of the experiments as the front moved down from the top of the cell. In the pictures white corresponds to blue (oxidized) regions of the solution, while black corresponds to red. The pictures show that in the cells of smaller width we can identify the waves of the oscillating reaction. In cells of larger width because of convection, the usual pure reaction–diffusion fronts cannot be identified. Pictures were taken 3–4 min after the induction period. One can see that, even in the case of the cell with 0.1 mm width, convection occurred. Figure 7 shows the formation of the reaction front as time goes on in the case of the 1 mm wide cell. It can be seen that after the solution at the open end of the tube becomes red, little “fingers” start to propagate downward and become wider.

Ascending Fronts. Figure 8 shows images when the front moved upward. In this case the time data appearing above the pictures also indicate time (in minutes) passed after the induction period. In the pictures of Figure 8 the reaction fronts moving upward are also curved but not as much as the ones downward.

Discussion

In this system the thermal density change ($\Delta\rho_T < 0$) and the isothermal density change ($\Delta\rho_c > 0$) have the opposite sign. According to the Pojman–Epstein model,³ double-diffusive convection should occur as in the iron(II)–nitric acid system^{1,5} and in the bromate–sulfite system;¹² that is, both the ascending and the descending fronts propagate faster than a pure reaction–

diffusion front. This is shown in Figure 4, which—as far as we know—is the first “pumpkin-shaped” curve of a BZ system. Our results are in good agreement with the results of Fujieda et al.;²¹ that is the propagation of the descending front is the fastest, while the ascending front is the slowest. Figure 8 shows that the ascending fronts in cells are slightly curved. The descending fronts have a significant parabolic shape in smaller cells (Figure 6), and formation of fingers occurs in broader cells; these are predicted by the Pojman–Epstein model.

Conclusion

If we compare these results with the results of Masere et al.⁷ and Wu et al.,²⁴ we can conclude that in this system simple convection does not occur, and Wu et al.’s model is not directly applicable. This is consistent for fronts exhibiting double-diffusive convection, but this is the first example of double-diffusive convection with waves.

Acknowledgment. This work was supported by the National Scientific Research Fund of Hungary (OTKA Grants 1725, F 4024, F 016166, and T 19254). A.K. also thanks the Universitas Foundation of Kereskedelmi Bank RT, Debrecen, for support. We are very grateful for helpful discussions with Professors Miklós Orbán and Krisztina Kurin-Csörgei.

References and Notes

- (1) Bazsa, G.; Epstein, I. R. *J. Phys. Chem.* **1985**, *89*, 3050.
- (2) Nagypál, I.; Bazsa, G.; Epstein, I. R. *J. Am. Chem. Soc.* **1986**, *108*, 3635.
- (3) Pojman, J. A.; Epstein, I. R. *J. Phys. Chem.* **1990**, *94*, 4966.
- (4) Pojman, J. A.; Epstein, I. R.; McManus, T.; Showalter, K. *J. Phys. Chem.* **1991**, *95*, 1299.
- (5) Pojman, J. A.; Epstein, I. R.; Nagy, I. *J. Phys. Chem.* **1991**, *95*, 1306.
- (6) Vasquez, D. A.; Edwards, B. F.; Wilder, J. W. *Phys. Rev. A* **1991**, *43*, 6694.
- (7) Masere, J.; Vasquez, D. A.; Edwards, B. F.; Wilder, J. W.; Showalter, K. *J. Phys. Chem.* **1994**, *98*, 6505.
- (8) Chinake, C. R.; Simoyi, R. H. *J. Phys. Chem.* **1994**, *98*, 4012.
- (9) Nagy, I. P.; Keresztessy, A.; Pojman, J. A. *J. Phys. Chem.* **1995**, *99*, 5385.
- (10) Nagy, I. P.; Pojman, J. A. *J. Phys. Chem.* **1993**, *97*, 3443.
- (11) Nagy, I. P.; Keresztessy, A.; Pojman, J. A.; Bazsa, G.; Noszticzius, Z. *J. Phys. Chem.* **1994**, *98*, 6030.
- (12) Keresztessy, A.; Nagy, I. P.; Bazsa, G.; Pojman, J. A. *J. Phys. Chem.* **1995**, *99*, 5379.
- (13) Plesser, T.; Wilke, H.; Winters, K. H. *Chem. Phys. Lett.* **1992**, *200*, 158.
- (14) Mattheissen, K.; Wilke, H.; Müller, S. C. *Phys. Rev. E* **1996**, *53*, 6056.
- (15) Miike, H.; Müller, S. C.; Hess, B. *Phys. Rev. Lett.* **1988**, *61*, 2109.
- (16) Miike, H.; Müller, S. C.; Hess, B. In *Cooperative Dynamics in Physical Systems*; Takayama, H., Ed.; Springer-Verlag: Berlin, 1989; pp 328–329.
- (17) Miike, H.; Yamamoto, H.; Kai, S.; Müller, S. C. *Phys. Rev. E* **1993**, *48*, 1627.
- (18) Miike, H.; Müller, S. C. *Chaos* **1993**, *3*, 21.
- (19) Plesser, T.; Miike, H.; Müller, S. C.; Winters, K. H. In *Spatial Inhomogeneities and Transient Behavior in Chemical Kinetics*; Gray, P., Nicolis, G., Baras, F., Borckmans, P., Scott, S. K., Ed.; Manchester University Press: Manchester, U.K., 1990; pp 383–391.
- (20) Menzinger, M.; Tzalmona, A.; Armstrong, R. L.; Cross, A.; Lemaire, C. *J. Phys. Chem.* **1992**, *96*, 4725.
- (21) Fujieda, S.; Mogamia, Y.; Furuya, A.; Zhang, W.; Araiso, T. *J. Phys. Chem. A* **1997**, *101*, 7926.
- (22) Otowska, M.; Kawczynski, A. L. *Pol. J. Chem.* **1992**, *66*, 697.
- (23) Kawczynski, A. L.; Otowska, M. *Z. Phys. Chem.* **1994**, *186*, 171.
- (24) Wu, Y.; Vasquez, D. A.; Edwards, B. F.; Wilder, J. W. *Phys. Rev. E* **1995**, *51*, 1119.
- (25) Farage, V. J.; Janjic, D. *Chem. Phys. Lett.* **1982**, *88*, 301.
- (26) Kurin-Csörgei, K.; Szalai, I.; Molnár-Perl, I.; Körös, E. *React. Kinet. Catal. Lett* **1994**, *53*, 115.
- (27) Kurin-Csörgei, K.; Szalai, I.; Körös, E. *React. Kinet. Catal. Lett.* **1995**, *54*, 217.
- (28) Kurin-Csörgei, K.; Zhabotinsky, A. M.; Orbán, M.; Epstein, I. R. *J. Phys. Chem.* **1996**, *100*, 5393.